This article has been accepted for publication in a future issue of this journal, but has not been fully edited. Content may change prior to final publication. Citation information: DOI 10.1109/TAP.2018.2876712, IEEE Transactions on Antennas and Propagation

Modeling the Impact of Rain and Clouds on Earth-Space Site Diversity Systems

Lorenzo Luini, *Senior Member*, *IEEE*, Carlo Riva, *Senior Member*, *IEEE*, Luis Emiliani, *Member*, *IEEE*, James Nessel

***Abstract*— A statistical model to predict the effects of both rain and clouds on Earth-space site diversity communication systems is presented. The methodology relies on the assumption, already widely considered in the literature, that both rain and cloud induced attenuations can be separately modelled, both in space and time, using log-normal distributions. The model is preliminarily tested against joint statistics of rain and cloud attenuation derived from the propagation dataset collected in three Italian sites (Spino d'Adda and Milan, in the North, and Tito Scalo, in the South) during the ongoing Alphasat Aldo Paraboni propagation experiment. Although additional experimental data including attenuation induced by rain and clouds are required to further assess the accuracy of the proposed site diversity model, the obtained results, both for short (~ 20 km) and large (~ 760 km) site separation distance, are definitely encouraging and suggest that the proposed model is a step towards providing a more comprehensive and accurate prediction of tropospheric impairments for near future high frequency Earth-space systems implementing site diversity.**

***Index Terms*— Electromagnetic propagation, rain effect, cloud effect, satellite communications.**

I. Introduction

In satellite communications (SatComs), site diversity is a fade mitigation technique resulting from the combination of the signals received from two or more ground terminals, or in the dynamic selection of the least-faded signal, in order to maximize the overall system Quality of Service (e.g. availability and/or throughput). Site diversity relies on the spatial inhomogeneity of the attenuation induced by tropospheric constituents, with rain playing the most relevant role: the larger the separation distance *D* between the stations, the higher the spatial decorrelation of the attenuation, and the greater the advantage that the diversity system will bring. That said, the larger *D* is, the more complex the operation of the whole system will be. With this in mind, one of the key questions to answer when approaching the design of a site diversity system is to optimize *D*, i.e. determine the probability of two (or more) stations jointly exceeding a given attenuation value as a function of *D*, such that the system's Quality of Service goals are met.

Site diversity is increasingly relevant in the context of high throughput satellites and multi-beam payloads. In satellite architectures with a static mapping between a gateway station and a series of serviced beams, a gateway outage event will have a large impact in terms of lost capacity and number of unserved users. As advanced payloads with digital processing on board are proposed, supporting terabit-per-second throughputs and using a mix of Q and Ka bands for gateway and user services, the need to deploy "smart" gateway diversity concepts increases [1]. This becomes evident when the magnitude of the atmospheric attenuation at Q band – typically exceeding 40 dB for 0.01% of the yearly time at 39.6 GHz [2] – is considered. Accurate modelling of the statistics involved in a site diversity analysis is a must to support, for example, the investment decision on a diversity gateway network and to determine the optimum deployment conditions for each member of the gateway network.

To this aim, several models to calculate joint probability distributions of tropospheric impairments have been proposed. While a comprehensive list of the available models would be long, it is worth mentioning recent examples such as the semi-empirical method in [3], the statistical approach in [4] and the model adopted by ITU-R [5], which allows the calculation of the joint distribution for both balanced and unbalanced systems. An alternative to the aforementioned closed-form approaches, is the use of space-time simulations of attenuation fields to derive a single- and multiple-site attenuation distribution [6],[7],[8]. Though very useful and flexible, this approach is characterized by higher complexity in the underlying methods, and is suitable to derive information beyond the joint distributions, such as spatially and temporally correlated time series of the attenuation. On the contrary, statistical approaches are simpler to use and apply, but usually address only the contribution of rain attenuation. As the operational frequency increases, the impact of other tropospheric phenomena such as clouds should be taken into due account to provide a more accurate and reliable model-based system design.

In order to address this issue, this contribution presents a model aimed at predicting the joint distribution of attenuation, including the effects of both rain and clouds on SatCom systems, aimed at improving the models available for planning a site diversity system. The model is an extension of the

Manuscript received XXXX.

Lorenzo Luini and Carlo Riva are with the Dipartimento di Elettronica, Informazione e Bioingegneria, Politecnico di Milano, Piazza Leonardo da Vinci 32, 20133, Milano, Italy, and with the Istituto di Elettronica e di Ingegneria dell'Informazione e delle Telecomunicazioni (IEIIT), Consiglio Nazionale delle Ricerche, Via Ponzio 34/5, Milano 20133, Italy (e-mail: lorenzo.luini@polimi.it).

Luis Emiliani is with SES S.A., Luxembourg (e-mail: ldemiliani@ieee.org).

James Nessel is with NASA Glenn Research Center (e-mail: james.a.nessel@nasa.gov).

This article has been accepted for publication in a future issue of this journal, but has not been fully edited. Content may change prior to final publication. Citation information: DOI 10.1109/TAP.2018.2876712, IEEE Transactions on Antennas and Propagation

mathematical framework underpinning the currently recommended ITU-R methodology to estimate joint rain attenuation statistics [5]: based on the assumption that both rain and cloud attenuation are log-normally distributed, the effects of both constituents are combined on a statistical basis to evaluate joint attenuation statistics. The remainder of the paper is structured as follows: Section II describes in detail the site diversity model including the contribution of both rain and clouds; Section III offers a preliminary validation of the model using, as reference, the data collected in the frame of the Alphasat Aldo Paraboni propagation experiment from three sites located in Italy (Spino d'Adda and Milano, in the North, and Tito Scalo, in the South). Finally, Section IV draws conclusions.

II. Site Diversity Model for Rain and Clouds

A. Rationale of the Model

The model proposed in this contribution to evaluate the impact of both rain and clouds on Earth-space site diversity systems originates from the theoretical framework outlined in [9] (and adopted by ITU-R in [5]), which proposes a log-normal model, valid both in space and time, to describe the statistical behavior of rain attenuation, A_R. This concept is here extended to the effects induced by clouds on Earth-space links, on the basis of preceding works indicating that the integrated liquid water content in clouds, L (and hence the associated attenuation, A_C), follows a log-normal distribution [10],[11],[12],[13]. Under this well-established assumption, as shown in [9] and [5], and as further explained in Section II.B below, the attenuation due to clouds (rain) concurrently impairing two Earth-space links can be calculated analytically by exploiting the well-known properties of log-normal random variables. Finally, the joint attenuation due to clouds and rain are combined on a statistical basis in order to assess the impact of both constituents on Earth-space systems implementing site diversity.

B. The Theoretical Framework

Let us consider two receivers both pointing at the same satellite, and installed at two sites, D kilometers apart, in a diversity configuration. Moreover, let A represent A_C or A_R, indistinctly, in order to simplify the notation (as mentioned, they are both assumed to be log-normally distributed). The joint probability that the attenuation along the path to the first site exceeds a_1 and the attenuation along the path to the second site exceeds a_2 is given by [5]:

$$P_J(A) = P(A_1 \geq a_1, A_2 \geq a_2) = P_{ing} \cdot P_{ed} \tag{1}$$

where P_{ing} is the joint probability that it is cloudy (or rainy) at both sites, while P_{ed} is the conditional joint probability that the attenuations exceed a_1 and a_2, respectively, given that it is cloudy (or rainy) at both sites. In other words, the dual-site attenuation statistics $P_J(A)$ originate from the combination of the probabilities associated to two independent processes, named the *conditioning process* and *conditioned process*, respectively [9]. As for the former, P_{ing} can be expressed in terms of the bivariate normal distribution taking into account both sites [5]:

$$P_{ing} = \frac{1}{2\pi\sqrt{1-\rho_{ing}^2}} \int_{X_1}^{\infty}\int_{X_2}^{\infty} \exp\left[-\left(\frac{x_1^2 - 2\rho_{ing}^2 x_1 x_2 + x_2^2}{2(1-\rho_{ing}^2)}\right)\right] dx_1\, dx_2 \tag{2}$$

where ρ_{ing} is the spatial correlation coefficient between the two sites for the conditioning process, which regulates the joint probability to have clouds or rain affecting both links [9]. The thresholds X_i for site i with probability to have clouds or rain $P_i^{C/R}$ is determined by solving (Q is the complementary cumulative normal distribution):

$$P_i^{C/R} = Q(X_i) = \frac{1}{\sqrt{2\pi}} \int_{X_i}^{\infty} \exp\left(\frac{x^2}{2}\right) dx \tag{3}$$,

which, inverted, leads to:

$$X_i = Q^{-1}(P_i^{C/R}) \tag{4}$$

As for the conditioned process, under the hypothesis that the attenuation A along a link is log-normally distributed, both in space and time, the conditioned probability can be expressed through [5]:

$$P_{ed} = \frac{1}{2\pi\sqrt{1-\rho_{ed}^2}} \int_{B_1}^{\infty}\int_{B_2}^{\infty} \exp\left[-\left(\frac{b_1^2 - 2\rho_{ed}^2 b_1 b_2 + b_2^2}{2(1-\rho_{ed}^2)}\right)\right] db_1\, db_2 \tag{5}$$

where ρ_{ed} is the spatial correlation coefficient between the two sites for the conditioned process, which regulates the amount of cloud or rain attenuation jointly affecting both links [9]. Moreover,

$$b_i = \ln A_i \quad \text{and} \quad B_i = \frac{\ln a_i - \mu_i}{\sigma_i} \tag{6}$$.

where μ_i and σ_i are the average and standard deviation values of b_i, respectively.

C. Model Parameterization for Rain and Clouds

The theoretical framework outlined above needs to be parameterized differently for rain and clouds; indeed, though the two processes are tightly linked from a meteorological standpoint, they also show marked differences: rain induces on electromagnetic waves much stronger attenuation than clouds, and, in addition, the spatial decorrelation trend for rain is much steeper than that of clouds [10].

This article has been accepted for publication in a future issue of this journal, but has not been fully edited. Content may change prior to final publication. Citation information: DOI 10.1109/TAP.2018.2876712, IEEE Transactions on Antennas and Propagation

1) *Rain*: The parameterization of the site diversity model for rain is derived from [9],[5], in which the correlation coefficients for the conditioning and the conditioned processes are defined as a function of the site separation distance $D \leq 1000$ km:

$$\rho_{ing}^{R} = 0.7e^{-D/60} + 0.3e^{-(D/700)^2} \quad (7)$$

$$\rho_{ed}^{R} = 0.94e^{-D/30} + 0.06e^{-(D/500)^2} \quad (8)$$

$X_i = R_i$ is derived from (4), where P_i^R, the probability to have rain in site i, can be globally extracted, for instance, from recommendation ITU-R P.837-7 [14]. Finally, μ_i and σ_i are calculated by fitting the local rain attenuation statistics, $P(A_R)$, which, in turn, if not available from measurements, can be estimated, for example, using the model included in recommendation ITU-R P.618-12 [5]. This approach is exemplified in Fig. 1, which depicts the rain attenuation statistics, both for a single- and a dual-site Earth-space system, estimated using the model described above; all input data were extracted from the latest ITU-R recommendations (e.g. from ITU-R P.837-7 for rain rate statistics [14]). The results are relative to the area of Milan, Italy, where two ground stations are installed to receive the beacon signals emitted by the Aldo Paraboni payload onboard the geosynchronous satellite Alphasat (more details on such an experiment are provided in Section III.A below). Table I lists the details on the Alphasat beacon signals and on ground terminals installed in the area of Milan, Italy, specifically in Spino d'Adda and in Politecnico di Milano main campus within the city. As shown in the last row of the table, the site separation distance is 21.7 km, which is sufficient to provide quite a significant benefit from the implementation of site diversity schemes [16]. This is clearly shown in Fig. 1: rain attenuation is expected to exceed 18.4 dB at 39.4 GHz for 0.1% of the yearly time using a single link, and 7 dB using the two sites in diversity configuration.

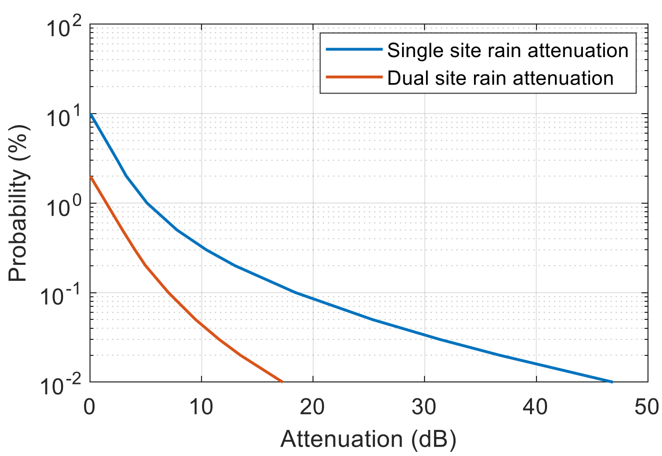

Fig. 1. Single- and dual-site (Milan and Spino d'Adda) rain attenuation statistics calculated using the site diversity model outlined in this Section and ITU-R recommendations fed with the electrical/geometrical characteristics listed in Table I (f = 39.4 GHz).

TABLE I. DETAILS ON THE ALPHASAT BEACON SIGNALS AND ON THE GROUND TERMINALS INSTALLED IN ITALY.

	Spino d'Adda	Milan	Tito Scalo
Elevation angle	35.6°	35.6°	42.1°
Latitude **Longitude**	45.40° N 9.48° E	45.47° N 9.23° E	40.58° N 15.72° E
Altitude	81 m	137 m	765 m
Receiver frequencies	19.7 and 39.4 GHz		
Beacon signal polarization	Linear vertical at 19.7 GHz Linear 45°-tilted at 39.4 GHz		
Distance between the sites	Spino d'Adda-Milan = 21.7 km Spino d'Adda-Tito Scalo = 760 km		

2) *Clouds:* Clouds have been extensively studied in [10], in which the integrated liquid water content L is shown to be log-normally distributed and, in addition, ρ_{ed}^{C} is calculated from MODIS-derived global maps of L. The same MODIS dataset (please refer to Section III.A in [10] for more details on such data) was used here to extend the calculation of ρ_{ed}^{C} up to site separation distances of 1000 km, in accordance with the rain correlation coefficients in (7) and (8). The conditioned correlation index for clouds obtained from MODIS data is accurately fitted by the following analytical expression:

$$\rho_{ed}^{C} = 0.33e^{-D/8.2} + 0.67e^{-D/463.1} \quad (9)$$

Furthermore, the same dataset was used to calculate also the conditioning correlation coefficient, whose trend with the site separation distance is well approximated by the following exponential law:

$$\rho_{ing}^{C} = 0.36e^{-D/10.1} + 0.53e^{-D/165.8} + 0.1e^{-D/776.9} \quad (10)$$

Fig. 2 shows both ρ_{ing}^{C} and ρ_{ed}^{C} for clouds, along with the fitting expressions in (9) and (10). For the sake of completeness, also ρ_{ing}^{R} and ρ_{ed}^{R} for rain are reported in Fig. 3: the comparison of the two figures clearly confirms that the spatial decorrelation of rain is steeper than that of clouds.

~~Although~~ ρ_{ing}^{C} and ρ_{ed}^{C}, as well as ρ_{ing}^{R} and ρ_{ed}^{R}, are valid for temperate climates as they were obtained from data collected over Europe[1], and their applicability in other climatic regions should be assessed with further availability of data~~they are assumed to be applicable worldwide, because the average spatial correlation of clouds and rain is not expected to change dramatically in different climates~~.

[1] ρ_{ing}^{C} and ρ_{ed}^{C} were obtained using MODIS-derived integrated liquid water content [10]; ρ_{ing}^{R} and ρ_{ed}^{R} were obtained using radar-derived and raingauge-derived rain rate measurements collected in Italy [9], but exhibiting spatial correlation features that were found to be similar across various sites in Europe [17])

This article has been accepted for publication in a future issue of this journal, but has not been fully edited. Content may change prior to final publication. Citation information: DOI 10.1109/TAP.2018.2876712, IEEE Transactions on Antennas and Propagation

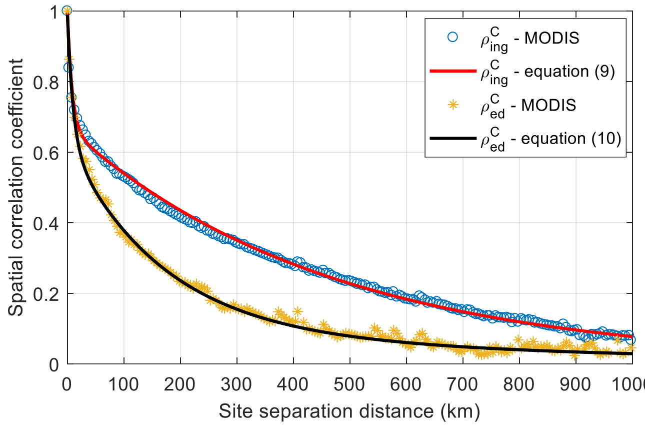

Fig. 2. Spatial correlation coefficient for the conditioning process, ρ_{ing}^{C} (blue circles), and the conditioned process, ρ_{ed}^{C} (yellow stars), for clouds, both derived from MODIS integrated liquid water content data. Also reported in the figure are the analytical expressions fitting the data (red and black solid lines, respectively).

In order to apply the site diversity model for clouds, $X_i = L_i$ is derived from (4), where P_i^C, the probability to have clouds over site i, can be extracted from recommendation ITU-R P.840-7 [15], which provides, on a global basis, the statistics of cloud integrated liquid water content L. The same recommendation can be used to estimate the complementary cumulative distribution function (CCDF) of the cloud attenuation, $P(A_C)$, from which, in turn, μ_l and σ_l can be obtained through curve fitting.

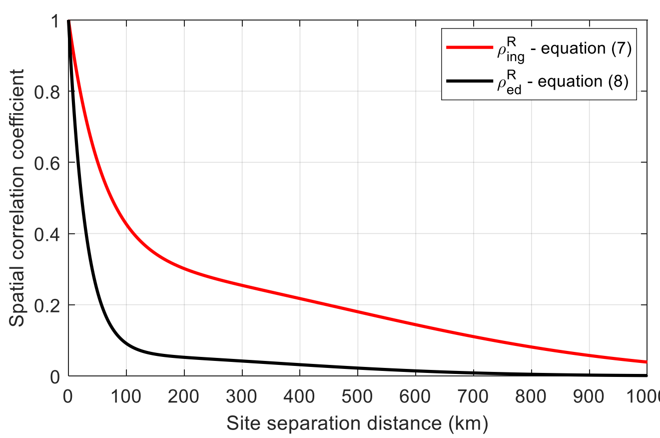

Fig. 3. Spatial correlation coefficients for the conditioning process, ρ_{ing}^{R} (red line), and the conditioned process, ρ_{ed}^{R} (black line), for rain, both extracted from [9].

Fig. 4 depicts, as an example, the cloud attenuation statistics, both for a single- and a dual-site Earth-space system, estimated using the model described in this Section and again the geometrical/electrical link characteristics listed in Table I (Spino d'Adda-Milan, f = 39.4 GHz). As expected, given the large spatial correlation of clouds and their quite low impact at Q band, the advantage deriving from implementing site diversity is quite limited as for what concerns the effect of clouds. Nevertheless, it is worth noticing that the probability that clouds affect the system (attenuation higher than 0 dB) decreases from approximately 50% to roughly 30% when the satellite signal is received at one site and at two sites in diversity configuration, respectively.

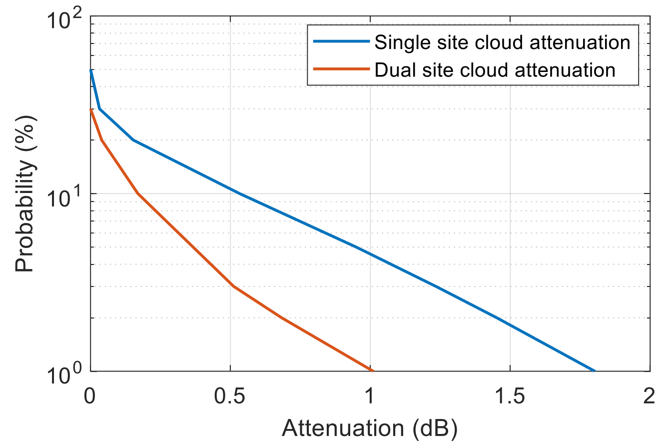

Fig. 4. Single- (blue line) and dual-site (red line) cloud attenuation statistics calculated using the site diversity model introduced in this Section and ITU-R recommendations fed with the electrical/geometrical characteristics listed in Table I (f = 39.4 GHz).

D. Joint Effect of Rain and Clouds

The combination of the two models described in Sections II.C aiming at assessing the effects of clouds and rain on site diversity systems is achieved by resorting to recommendation ITU-R P.618-13, which defines an analytical expression to statistically combine the attenuation due to rain, clouds, gases and scintillations. If the last two contributions are neglected, the formula reduces to the simple summation of A_R and A_C on equiprobable basis, i.e. [5]:

$$A_{RC}(P) = A_R(P) + A_C(P) \tag{11}$$

where P is the CCDF exceedance probability.

Fig. 5 shows the application of (11), both on the single- and on the dual-site statistics, starting from the A_R and A_C curves included in Fig. 1 and Fig. 4, respectively (curves labeled 'rain plus cloud attenuation'). Obviously, the contribution of clouds is quite limited if compared to that of rain, which emerges by comparing the red and green curves in Fig. 5 (the latter, relative to the dual site system but associated to rain-only attenuation, is extracted from Fig. 1); nevertheless, the proposed model is a step towards providing a more comprehensive assessment of the impact of the troposphere on high-frequency Earth-space systems implementing site diversity.

This article has been accepted for publication in a future issue of this journal, but has not been fully edited. Content may change prior to final publication. Citation information: DOI 10.1109/TAP.2018.2876712, IEEE Transactions on Antennas and Propagation

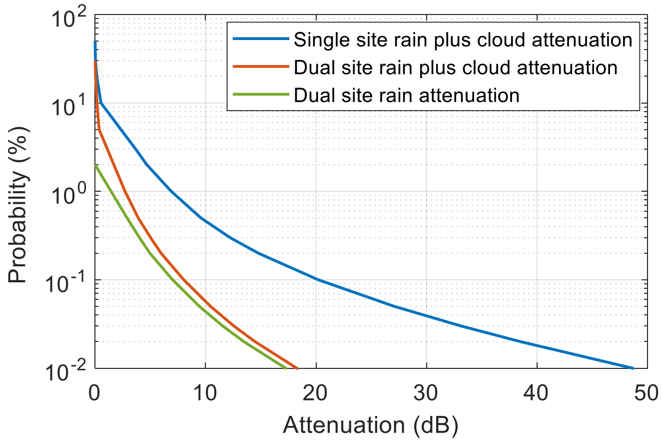

Fig. 5. Single- (blue line) and dual-site (red line) cloud plus rain attenuation statistics calculated by combining the site diversity models for the two constituents and using the electrical/geometrical characteristics listed in Table I (Spino d'Adda-Milan, f = 39.4 GHz). For the sake of comparison, also the dual-site rain-only attenuation statistics are included (green line, extracted from Fig. 1).

III. Preliminary Model Accuracy Assessment

A thorough evaluation of the accuracy of the rain-cloud attenuation diversity model is cumbersome, given the lack of experimental attenuation statistics that include the effects induced by both constituents. Notwithstanding this, we provide in this Section at least an indication of the model validity by exploiting the propagation dataset collected in Spino d'Adda, Milan and Tito Scalo in the frame of the Alphasat Aldo Paraboni propagation experiment.

A. *The Alphasat Aldo Paraboni Propagation Experiment*

The space segment of the Aldo Paraboni propagation experiment consists of two beacons operating at 19.7 GHz and 39.4 GHz and covering the whole of Europe. The payload development was supported by the Italian Space Agency (ASI) and executed by the European Space Agency [18]. The Aldo Paraboni payload is embarked aboard the Alphasat satellite (hosting the main commercial payload of Inmarsat), which was successfully launched on the 25th of July, 2013.

As for the ground segment, ASI, with the support of Politecnico di Milano as Principal Investigator of the propagation experiment, committed Space Engineering to manufacture and deploy two identical propagation ground stations in Italy; the first one is located in Tito Scalo (near Potenza, South of Italy) and the second one in Spino d'Adda (near Milan, North of Italy). Both stations are equipped with a monopulse auto tracking system and measure the co-polar signal at 19.7 and 39.4 GHz (and the cross-polar signal at 39.4 GHz) with a 4.2 m diameter antenna at an average elevation angle of 42.1° (Tito Scalo) and 35.6° (Spino d'Adda). A 16-Hz sampling rate is implemented to properly characterize scintillation effects. The receiver dynamic range is almost 60 dB. A profiler radiometer (RPG-HATPRO), a tipping bucket rain gauge and an ancillary meteorological station complete the equipment of both stations. Fig. 6 shows the ground station installed at Spino d'Adda (top).

NASA Glenn Research Center joined the Alphasat Aldo Paraboni propagation experiment in 2014 by developing and installing a Ka/Q-band fast Fourier transform beacon receiver at Politecnico di Milano campus in Milan, Italy [19]. The system consists of a 1.2 m Ka-band and a 0.6 m Q-band Cassegrain antennas employing synchronous open-loop tracking to follow the Alphasat satellite along its inclined equatorial orbit. An 8-Hz sampling rate is implemented, with a dynamic range (1-Hz measurement bandwidth) of approximately 45 dB. A weather station with an optical disdrometer is also installed to characterize rain drop size distribution for correlation with physically-based models. Fig. 6 shows the ground station installed in Milan (bottom).

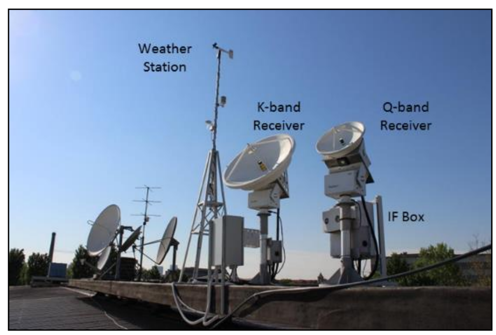

Fig. 6. ASI (top) and NASA (bottom) Alpahsat Ka/Q-band beacon receivers at Spino d'Adda experimental station (same equipment installed at Tito Scalo) and at Politecnico di Milano premises, respectively.

B. *Data processing and results*

One year of measurements (from January 1st, 2015 to December 31st, 2015), collected by the three Italian ground stations were processed to obtain attenuation statistics. For that year, the probability to have rain attenuation in the three sites is approximately 8% (Milan), 7.5% (Spino d'Adda) and 4.5% (Tito Scalo).

As a first step, for all stations, the received power was turned into total attenuation A_T (i.e. due to all the atmospheric constituents) using the method outlined in [20]. In synthesis, the procedure relies on the prediction of the clear-sky total attenuation (i.e. including only the effects of clouds and gases) using the Liebe's MPM93 mass absorption model [21] and vertical atmospheric profiles from radiosonde observation collected at Milano Linate Airport (quite close to both Northern sites), and numerical weather prediction products,

This article has been accepted for publication in a future issue of this journal, but has not been fully edited. Content may change prior to final publication. Citation information: DOI 10.1109/TAP.2018.2876712, IEEE Transactions on Antennas and Propagation

made available by the European Centre for Medium-range Weather Forecast.

Afterwards, the attenuation induced on the links by gases, A_G, was subtracted by resorting to the models adopted by ITU-R in recommendation P.676 to estimate the fade due to oxygen, A_{OX}, and water vapor, A_{WV}. Specifically, we have implemented and used the simplified models included in Annex 2 of P.676-10 [22], which express the total gaseous attenuation along the path as:

$$A_G = \frac{\gamma_{OX}\, h_{OX}^0 + \gamma_{WV}\, h_{WV}^0}{\sin\theta} \tag{12}$$

where $\gamma_{OX/WV}$ is the gaseous specific attenuation (dB/km) at ground, level, while $h_{OX/WV}^0$ is the associated equivalent height (km), which takes into account the exponential decay of the specific attenuation with height (both for oxygen [23] and water vapor [24]). Finally, θ is the link elevation angle. As explained in [22], the specific attenuations and equivalent heights in (12) depend on the ground pressure, P, temperature, T, and relative humidity, RH, which are measured at the experimental stations with 1-minute sampling time. As an example of the application of (12), Fig. 7 depicts the tropospheric attenuation measured in Spino d'Adda at 39.4 GHz. More specifically, shown in the figure are the total attenuation A_T (i.e. including all the effects but scintillations, which are removed using a low-pass filter), the gaseous attenuation $A_G = A_{WV} + A_{OX}$, estimated using Annex 2 of recommendation ITU-R P.676-10, and the attenuation due to rain and clouds $A_{RC} = A_T - A_G$. As is clear from Fig. 8, reporting the trend of the rain rate for the same day, the link is affected by a moderate precipitation event (roughly between 8 and 16 UTC), while before and after it, some non-rainy clouds cause an attenuation up to 1 dB at 39.4 GHz.

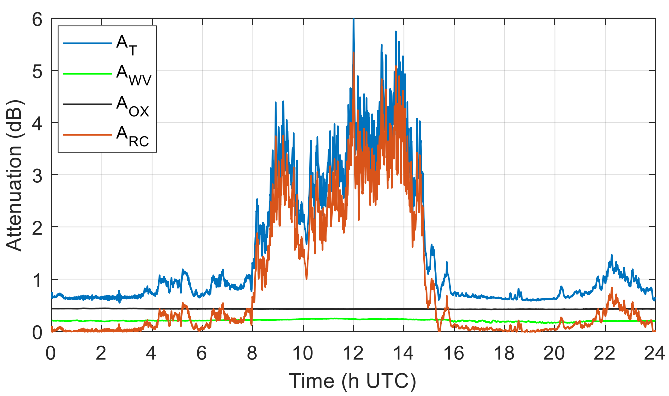

Fig. 7. Atmospheric attenuation measured on the 24th of February, 2015, in Spino d'Adda, at 39.4 GHz.

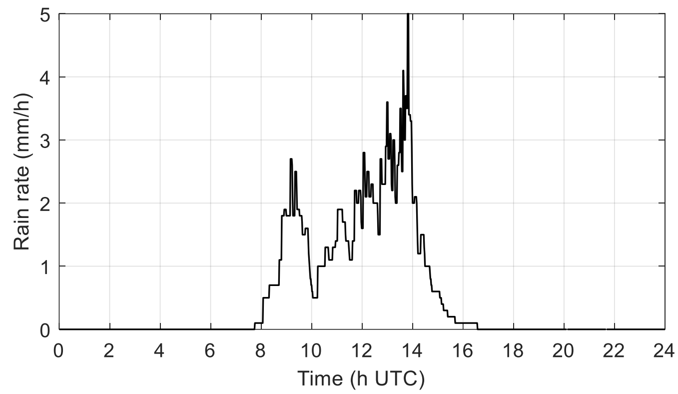

Fig. 8. Rain rate measured on the 24th of February, 2015, in Spino d'Adda (tipping-bucket raingauge).

Fig. 9 provides additional information on the 24th of February, 2015, by comparing A_{RC} measured in Spino d'Adda and in Milan: in general, for that day, the impairment caused by rain and clouds on the ground station in Milan is less pronounced than that in Spino d'Adda (the maximum value for A_{RC} is 2.65 dB and 5.34 dB, respectively). Also included in Fig. 9 is A_{RC} relative to a site diversity system taking advantage of both stations: the green dashed line is obtained by assuming a perfect switching between the two sites, i.e. by selecting, for every second, the minimum attenuation value. In fact, this is in line with the results provided by the clouds and rain site diversity model presented in Section II.

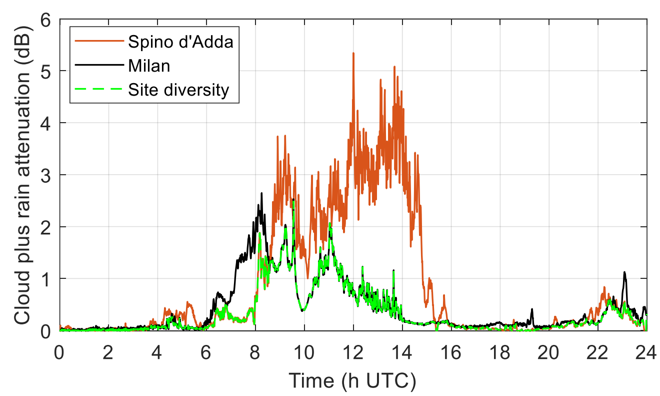

Fig. 9. Attenuation due to rain and clouds measured on the 24th of February 2015 in Spino d'Adda (red line) and Milan (black line) at f = 39.4 GHz. Also shown is A_{RC} (green dashed line) relative to a site diversity system.

Similar results are shown in Fig. 10 (f = 39.4 GHz), but for Spino d'Adda and Tito Scalo (4th of March 2015). Both sites are affected by the same extended rain front, but due to the large distance between the two sites, site diversity is even more effective: the maximum attenuation in Spino d'Adda and Tito Scalo is 24.7 dB and 12.4 dB, respectively, while for the site diversity system this values decreases to 8.3 dB.

This article has been accepted for publication in a future issue of this journal, but has not been fully edited. Content may change prior to final publication. Citation information: DOI 10.1109/TAP.2018.2876712, IEEE Transactions on Antennas and Propagation

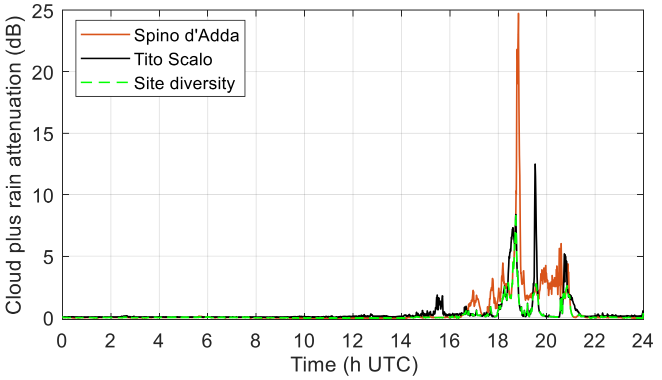

Fig. 10. Attenuation due to rain and clouds measured on the 4th of March 2015 in Spino d'Adda (red line) and Tito Scalo (black line) at f = 39.4 GHz. Also shown is A_{RC} (green dashed line) relative to a site diversity system.

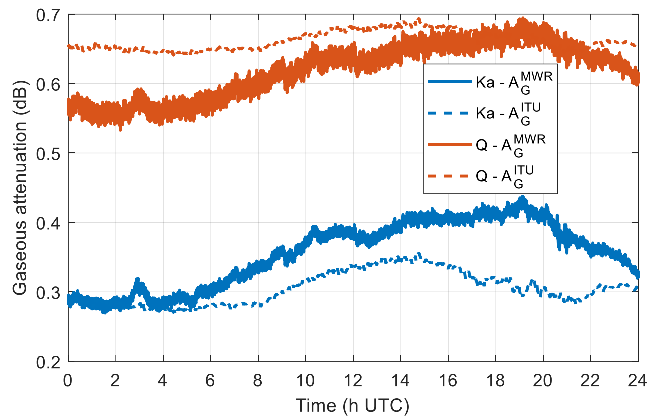

Fig. 11. Gaseous attenuation for Spino d'Adda (3rd of January, 2015), as estimated using the radiometer according to [26] and as predicted by the ITU-R P.676 models (both frequencies at 19.7 and 39.4 GHz).

The accuracy in estimating the attenuation due to both rain and clouds~~the attenuation due both to rain and clouds~~ using the procedure explained above is driven by the performance of the ITU-R P.676 models in predicting the path attenuation due to gases. In order to assess such an accuracy, we have compared the models' predictions with the gaseous attenuation estimated, in nonrainy conditions, by the radiometer installed in Spino d'Ad~~d~~da A_G^{MWR}, in turn obtained as:

$$A_G^{MWR} = A_T^{MWR} - A_C^{MWR} = A_T^{MWR} - a_L L \tag{13}$$

In equation (13), A_T^{MWR} is the total attenuation (at either of the beacon frequencies), calculated from the brightness temperature data of five radiometric channels (f = 23.84, 27.84, 31.4, 51.26 and 52.28 GHz) according to the procedure outlined in [26], while A_C^{MWR} is the cloud attenuation, calculated using the liquid water mass absorption coefficient a_L and the liquid water content integrated along the path L, also estimated using the same radiometric channels (see [27] for more details). Fig. 11 shows the gaseous attenuation as predicted by the ITU-R models and as estimated by the radiometer, at both bands, for the 3rd of January, 2018. These sample results show a satisfactory prediction accuracy, which is confirmed by the low mean value ($-2.6\cdot10^{-4}$ dB and 0.07 dB for the Ka and Q band, respectively) and low root mean square value (0.07 dB and 0.08 dB for the Ka and Q band, respectively) of the absolute prediction error, calculated on the data of the whole of 2015 (though considering only nonrainy conditions, for which radiometric retrievals are reliable [27]). Although these figures are not completely exhaustive, they provide at least an indication of the accuracy with which the attenuation due to both rain and clouds ~~the attenuation due both to rain and clouds~~ is obtained from the time series of beacon-derived total attenuation.

Fig. 12 depicts the CCDFs of the attenuation due to both rain and clouds the attenuation due to both rain and clouds ~~the attenuation due both to rain and clouds~~ as measured, at both bands, by the two receivers installed in Spino d'Adda and Milan (results relative to the whole year): as expected, because of the flat area where both sites lie and of their limited distance, the CCDFs are in good agreement; the differences are expected to be mainly ascribable to specific microclimatic features (Spino d'Adda is open countryside, Milan is a large city).

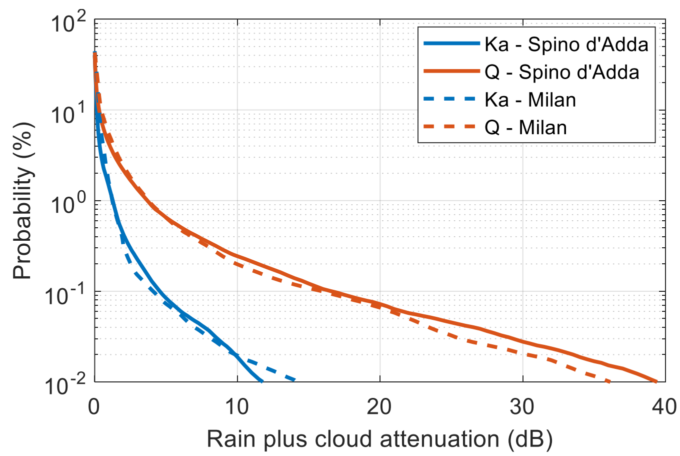

Fig. 12. CCDFs of the attenuation due to rain and clouds as measured, in 2015, at 19.7 GHz (blue lines) and 39.4 GHz (red lines), by the two receivers installed in Spino d'Adda (solid lines) and Milan (dashed lines).

Fig. 13 offers a hint of the accuracy of the site diversity model described in Section II, by comparing the CCDFs of joint rain and cloud attenuation as calculated, at both bands, by combining the data collected in Spino d'Adda and Milan (see Fig. 9) and as derived by the aforementioned model.

This article has been accepted for publication in a future issue of this journal, but has not been fully edited. Content may change prior to final publication. Citation information: DOI 10.1109/TAP.2018.2876712, IEEE Transactions on Antennas and Propagation

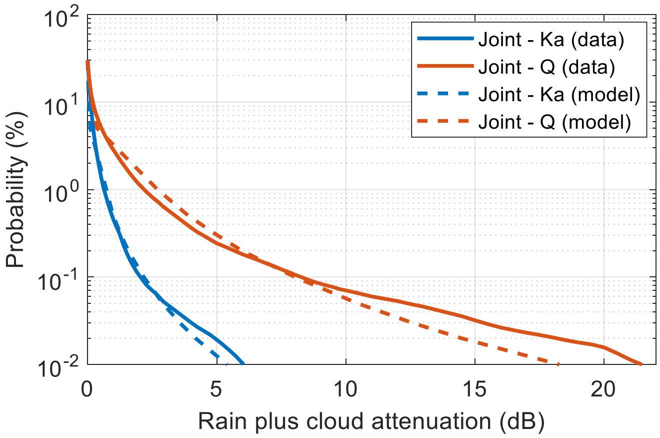

Fig. 13. CCDFs of the joint rain and cloud attenuation (solid lines) as calculated, at 19.7 GHz (blue lines) and 39.4 GHz (red lines), by combining the data collected in Spino d'Adda and Milan (D = 21.7 km). Also reported in the figure are the same curves (dashed lines) as derived by applying the site diversity models described in Section II.

The agreement between the model and the measurements is quite satisfactory across the whole range of exceedance probability (0.01% - 100%): both the data- and model-derived curves indicate that the probability to have clouds and rain affecting the dual-site diversity system reduces from roughly 50% to 30%.

Satisfactory accuracy for the model is obtained also for the stations in Spino d'Adda and Tito Scalo, which are far more distant (760 km): results, shown for both bands in Fig. 14, indicate again a good agreement between the model's predictions and the measurements, especially considering the large separation distance between the sites.

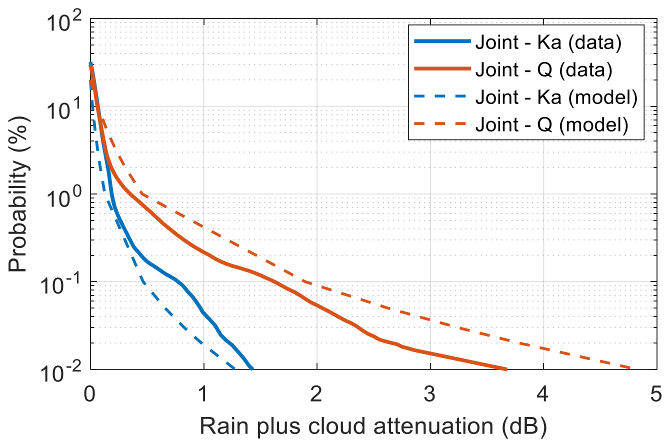

Fig. 14. CCDFs of the joint rain and cloud attenuation (solid lines) as calculated, at 19.7 GHz (blue lines) and 39.4 GHz (red lines), by combining the data collected in Spino d'Adda and Tito Scalo (D = 760 km). Also reported in the figure are the same curves (dashed lines) as derived by applying the site-diversity models described in Section II.

In order to quantify the model's prediction accuracy, we employ the following error figure [25]:

$$\psi(P)=\begin{cases}100\cdot\left(\dfrac{A_R(P)}{10}\right)^{0.2}\ln\left(\dfrac{A_P(P)}{A_R(P)}\right) & A_R(P)<10\text{ dB}\\ 100\cdot\ln\left(\dfrac{A_P(P)}{A_R(P)}\right) & A_R(P)\geq 10\text{ dB}\end{cases}\qquad(14)$$

In (14), $A_R(P)$ and $A_P(P)$ represent A_{RC}, both correspondent to probability level P, extracted respectively from the reference (measured data) and the estimated (model) CCDF of joint rain and cloud attenuation. Table II lists the average (E) and root mean square (RMS) values of $\psi(P)$ for both frequencies ($P \geq 10^{-2}$%).

TABLE II. AVERAGE (E) AND ROOT MEAN SQUARE (RMS) VALUES OF THE ERROR FIGURE.

	f = 19.7 GHz		**f = 39.4 GHz**	
	E	**RMS**	**E**	**RMS**
Spino d'Adda-Milan	-7.9%	17.5%	-2.3%	13.4%
Spino d'Adda-Tito Scalo	-18.2%	21.6%	17.2%	18.1%

Unfortunately, no additional experimental data including attenuation induced by rain and clouds are currently available to further assess the accuracy of the proposed site diversity model. Nevertheless, the results presented here are encouraging and suggest that the proposed model is a step towards providing a more comprehensive and accurate prediction of tropospheric impairments for near future high frequency Earth-space systems implementing site diversity.

IV. CONCLUSIONS

This paper presented a statistical model to predict the effects of both rain and clouds on Earth-space site diversity communication systems. The methodology relies on using the log-normal model, valid in space and time, to describe the statistical behaviour of both rain attenuation, A_R, and cloud attenuation, A_C, which, in turn, allows for a closed-form calculation of the joint attenuation statistics for any number of Earth-space links with separation distance $D \leq 1000$ km. To provide a prediction, the model requires as input the the trend of the spatial correlation of attenuation as a function of D, for both A_R and A_C. For rain, the correlation functions were taken from a previous work, while for clouds, analytical models are proposed based on fitting simple expressions on the data extracted from MODIS-derived cloud liquid water content maps.

In order to provide a preliminary assessment of the model validity, the propagation dataset collected in three Italian sites (Spino d'Adda and Milan, in the North, and Tito Scalo, in the South) during the ongoing Alphasat Aldo Paraboni propagation experiment (two beacon signals at 19.7 and 39.4 GHz) were processed first to isolate the effects of clouds and rain on the links, and afterwards to calculate joint statistics of rain plus cloud attenuation. Specifically, we have assumed two diversity schemes: a short scale one involving Spino d'Adda and Milan (21.7 km apart) and another one at large scale between Spino d'Adda and Tito Scalo (760 km). In both cases, the model has shown satisfactory accuracy in predicting joint rain and cloud attenuation statistics; as expected, better results were achieved at short scale (root mean square of the prediction error equal to 17.5% and 13.4% at 19.7 and 39.4 GHz, respectively) than at large scale (root mean square of the prediction error equal to 21.6% and 18.1% at 19.7 and 39.4 GHz, respectively). Although additional experimental data including attenuation induced by rain and clouds are required to further assess the accuracy of the proposed site diversity model and its applicability on global basis, these preliminary results are definitely encouraging and suggest that the proposed model is a step towards providing a more comprehensive and accurate prediction of tropospheric impairments for near future high frequency Earth-space systems implementing site diversity.

ACKNOWLEDGMENT

The authors would like to acknowledge the Agenzia Spaziale Italiana (ASI), in particular Giuseppe Codispoti, for supporting the Alphasat Aldo Paraboni propagation experiment.

This effort was partially sponsored by the Air Force Office of Scientific Research, Air Force Material Command, USAF, under grant number FA8655-13-1-3081. The U.S Government is authorized to reproduce and distribute reprints for Governmental purpose notwithstanding any copyright notation thereon.

REFERENCES

[1] A. Kyrgiazos, B. Evans, P. Thompson, M. Dervin, C. Baudoin, B. Garnier, "Gateway diversity for a future high throughput satellite system", in Proceedings of the 32nd AIAA International Communications Satellite Systems Conference. AIAA American Institute of Aeronautics and Astronautics, 2014.

[2] R. Polonio, C. Riva, "ITALSAT propagation experiment at 18.7, 39.6 and 49.5 GHz at Spino D'Adda: Three years of CPA statistics," *IEEE Trans. Antennas Propag.*, vol. 46, no. 5, pp. 631–635, May 1998.

[3] C. Nagaraja, I. E. Otung, "Statistical prediction of site diversity gain on earth-space paths based on radar measurements in the UK," *IEEE Transactions On Antennas And Propagation*, 60(1), pp. 247-256, 2012.

[4] S. N. Livieratos, C. I. Kourogiorgas, A. D. Panagopoulos, G. E. Chatzarakis, "On the Prediction of Joint Rain Attenuation statistics in Earth-Space Diversity Systems using Copulas," *IEEE Transactions on Antennas and Propagation*, 62(4), pp. 2250-2257, 2014.

[5] Propagation data and prediction methods required for the design of Earth-space telecommunication systems, document Rec. ITU-R 618-13, 2017.

[6] N. Jeannin, L. Féral, H. Sauvageot, L. Castanet, F. Lacoste, "A Large-Scale Space-Time Stochastic Simulation Tool of Rain Attenuation for the Design and Optimization of Adaptive Satellite Communication Systems Operating between 10 and 50 GHz," *International Journal of Antennas and Propagation*, vol. 2012, Article ID 749829, 16 pages, 2012.

[7] K. S. Paulson, L. Luini, I. D. Chinda, H. Basarudin, "Comparison of heterogeneous network rain fade simulation tools: global integrated network SIMulator and MultiEXCELL," *IET Microwaves, Antennas & Propagation*, 9(7), pp. 689-694, 2014.

[8] L. Luini, C. Capsoni, "MultiEXCELL: a new rain field model for propagation applications," *IEEE Transactions on Antennas and Propagation*, vol. 59, no. 11, Page(s): 4286 - 4300, November 2011.

[9] S. Bertorelli, A. Paraboni, "Simulation of Joint Statistics of Rain Attenuation in Multiple Sites Across Wide Areas Using ITALSAT Data," *IEEE Transactions on Antennas and Propagation*, vol. 53, no. 8, Page(s): 2611 - 2622, August 2005.

[10] L. Luini, C. Capsoni, "Modeling High Resolution 3-D Cloud Fields for Earth-space Communication Systems," *IEEE Transactions on Antennas and Propagation*, vol. 62, no. 10, Page(s): 5190 - 5199, October 2014.

[11] N. Jeannin, L. Feral, H. Sauvageot, L. Castanet, "Statistical Distribution of Integrated Liquid Water and Water Vapor Content From Meteorological Reanalysis," *IEEE Transactions on Antennas and Propagation*, vol. 56, no. 10, Page(s): 3350 - 3355, October 2008.

[12] N. K. Lyras, C. I. Kourogiorgas, A. D. Panagopoulos, "Cloud Attenuation Statistics Prediction From Ka-Band to Optical Frequencies: Integrated Liquid Water Content Field Synthesizer," *IEEE Transactions on Antennas and Propagation*, vol. 65, no. 1, Page(s): 319 - 328, January 2017.

[13] Tropospheric Attenuatuon Time Series Synthesis, document Rec. ITU-R 1853-1, 2012.

[14] Characteristics of precipitation for propagation modelling, document Rec. ITU-R 837-7, 2017.

[15] Attenuation due to clouds and fog, document Rec. ITU-R 840-7, 2017.

[16] L. Luini, C. Capsoni, "A Rain Cell Model for the Simulation and Performance Evaluation of Site Diversity Schemes," *IEEE Antennas and Wireless Propagation Letters*, vol. 12, No. 1, Page(s): 1327-1330, 2013.

[17] L. Luini, C. Capsoni: "Spatial correlation of rainfall over Europe investigated through statistical dependence index," *Electronics Letters*, Vol. 49, Issue 3, pp. 230-231, 31 January 2013.

[18] T. Rossi, M. De Sanctis, M. Ruggieri, C. Riva, L. Luini, G. Codispoti, E. Russo, G. Parca, "Satellite Communication and Propagation Experiments Through the Alphasat Q/V Band Aldo Paraboni Technology Demonstration Payload," *IEEE Aerospace and Electronic Systems Magazine*, Vol. 31, No. 3, Page(s): 18 – 27, March 2016.

[19] J. Nessel, J. Morse, M. Zemba, C. Riva, L. Luini, "Preliminary Statistics From the NASA Alphasat Beacon Receiver in Milan, Italy," pp. 1-5, EuCAP 2015, 12-17 April 2015, Lisbon, Portugal.

[20] J. Nessel, J. Morse, M. Zemba, C. Riva, L. Luini, "Performance of the NASA beacon receiver for the Alphasat Aldo Paraboni TDP5 propagation experiment," pp. 1-8, IEEE Aerospace Conference 2015, 7-14 March 2015, Big Sky, Montana, USA.

[21] H. J. Liebe, G. A. Hufford, M. G. Cotton, "Propagation modeling of moist air and suspended water/ice particles at frequencies below 1000 GHz," Proc. NATO/AGARD Wave Propagation Panel, 52nd meeting, No. 3/1-10, Mallorca, Spain, May 17-20, 1993.

[22] Attenuation by atmospheric gases, document Rec. ITU-R 676-10, 2013.

[23] L. Luini, C. Riva, "A Simplified Model to Predict Oxygen Attenuation on Earth-space Links," *IEEE Transactions on Antennas and Propagation*, vol. 65, no. 12, Page(s): 7217 - 7223, December 2017.

[24] L. Luini, C. Riva, "Improving the Accuracy in Predicting Water Vapor Attenuation at Millimeter-wave for Earth-space Applications," *IEEE Transactions on Antennas and Propagation*, vol. 64, no. 6, Page(s): 2487 - 2493, June 2016.

[25] Acquisition, presentation and analysis of data in studies of radiowave propagation, document Rec. ITU-R 311-15, 2015.

[26] L. Luini, C. Riva, R. Nebuloni, M. Mauri, J. Nessel, A. Fanti, "Calibration and Use of Microwave Radiometers in Multiple-site EM Wave Propagation Experiments," EuCAP 2018, 9-13 April 2018, London, UK.

[27] L. Luini, C. Riva, C. Capsoni, A. Martellucci, "Attenuation in non rainy conditions at millimeter wavelengths: assessment of a procedure," IEEE Transactions on Geoscience and Remote Sensing, pp. 2150-2157, Vol. 45, Issue 7, July 2007..